Response of Ni/4H-SiC Schottky barrier diodes to alpha-particle irradiation at different fluences

E. Omotoso[1,2], W.E. Meyer[1], F.D. Auret[1], M. Diale[1] and P.N.M. Ngoepe[1]

[1] *Department of Physics, University of Pretoria, Private Bag X20, Hatfield 0028, South Africa*

[2] *Departments of Physics, Obafemi Awolowo University, Ile-Ife, 220005, Nigeria*

Corresponding author e-mail address: ezekiel.omotoso@up.ac.za

ABSTRACT

Irradiation experiments have been carried out on 1.9×10^{16} cm^{-3} nitrogen-doped 4H-SiC at room temperature using 5.4 MeV alpha-particle irradiation over a fluence ranges from 2.6×10^{10} to 9.2×10^{11} cm^{-2}. Current-voltage (*I-V*), capacitance-voltage (*C-V*) and deep level transient spectroscopy (DLTS) measurements have been carried out to study the change in characteristics of the devices and free carrier removal rate due to alpha-particle irradiation, respectively. As radiation fluence increases, the ideality factors increased from 1.20 to 1.85 but the Schottky barrier height (SBH_{I-V}) decreased from 1.47 to 1.34 eV. Free carrier concentration, N_d decreased with increasing fluence from 1.7×10^{16} to 1.1×10^{16} cm^{-2} at approximately 0.70 μm depth. The reduction in N_d shows that defects were induced during the irradiation and have effect on compensating the free carrier. The free carrier removal rate was estimated to be 6480±70 cm^{-1}. Alpha-particle irradiation introduced two electron traps ($E_{0.39}$ and $E_{0.62}$), with activation energies of 0.39±0.03 eV and 0.62±0.08 eV, respectively. The $E_{0.39}$ as attribute related to silicon or carbon vacancy, while the $E_{0.62}$ has the attribute of Z_1/Z_2.

Keywords: DLTS, free carrier removal rate, carrier concentration, 4H-SiC, alpha-particle irradiation

1. Introduction

Metal-semiconductor (M-S) Schottky barrier diodes (SBDs) are widely used where diodes with low forward voltage drop, low capacitance and high switching speed are required [1]. This makes them ideal as rectifiers in photovoltaic systems and high-efficiency power supplies [2]. SBDs also have important uses in optoelectronics, high frequency and bipolar integrated circuits applications [3, 4]. The reliability of SBDs is influenced significantly by the quality of the M-S junction [5]. The performance of the devices can be quantified experimentally in terms of their ideality factor, Schottky barrier height (SBH), saturation

current, series resistance and free carrier concentration. Among these properties of the M-S interface, SBH plays a major role in the successful operation of many devices in transporting electrons across the M-S junction [6].

Silicon carbide (SiC) is a promising semiconductor with a wide bandgap of 3.26 eV [7], which has drawn the interest of many researchers due to its excellent properties such as high thermal conductivity, high breakdown field and high saturated drift velocity [8]. These characteristics make SiC a very good semiconductor capable of outperforming silicon in electronic devices for high-power, high-frequency and high-temperature applications [9], and is a key material for the next-generation photonics [10]. SiC is also good candidate for electronic devices used in harsh radiation environments such as in space, accelerator facilities and nuclear power plants [11-13].

In this study, we report the behaviour of 4H-SiC SBD prior to and after alpha-particle irradiation at different fluences. In order to use SiC in radiation hard devices, there is need to know the radiation response of SiC. Also, the fluence SiC can withstand before the characteristics of devices fabricated on it degrade and they start to malfunction, needs to be determined. Current-voltage (I-V), capacitance-voltage (C-V) and deep level transient spectroscopy (DLTS) have been carried out on SBDs to study the change in characteristics of the devices at different fluences.

2. Experimental procedure

The samples used for this work were cut from a nitrogen-doped n-type 4H-SiC wafer, double polished with the Si face epi layer. The substrate was doped by 1×10^{18} cm^{-3}, while the epi layer had a resistivity of 0.02 Ω-cm and a doping density of 1.9×10^{16} cm^{-3}. The wafers were supplied by CREE Res. Inc.

The samples were cut into smaller pieces (area of 8 mm^2) and degreased by boiling for 5 minutes each in trichloroethylene, acetone, methanol and followed by 1 minute rinse in de-ionized water. They were etched in 40% hydrogen fluoride for 30 seconds in order to remove the native oxide layer on the samples, then rinsed in de-ionized water, followed by blowing dry with nitrogen gas prior to thermally evaporation of nickel ohmic contacts onto the back surfaces (1.0×10^{18} cm^{-3} doped side) of the samples.

Nickel was used for both ohmic and Schottky contacts. Resistive evaporation was employed in both cases as it does not introduce measurable defects. The ohmic contact with a thickness of 2500 Å was deposited at a rate of 0.9 Ås^{-1}. The samples were annealed in a tube

furnace under flowing argon gas at 950℃ for 10 minutes to form nickel silicides [14] in order to minimize contact resistance. The samples were also cleaned in ultrasonic water bath for 3 minutes each in trichloroethylene, acetone and methanol followed by 1 minute rinsed in de-ionized H_2O after the annealing of the ohmic contact. Nickel Schottky contacts were resistively evaporated through a metal contact mask and had an area of 2.4×10^{-3} cm^2. The contacts of thickness 1000 Å were deposited at a rate of 0.5 Ås^{-1} under a vacuum of 3.0×10^{-5} mbar.

Samples were irradiated at room temperature and a fluence rate of 7.1×10^6 cm^{-2}-s^{-1} with alpha-particles of energy of 5.4 MeV from a 241-Am radionuclide source. The radioactive foils were placed on top of the SBDs in such a way that the emitted alpha-particles were directed on diodes. The alpha-particle fluence ranged from 2.6×10^{10} to 9.2×10^{11} cm^{-2} (i.e from 1 to 36 hr). The same SBD was used throughout the study and the radiation fluence quoted is the cumulative fluence over all radiations. A second SBD was irradiated and measured separately to check for repeatability.

Before in between irradiations, the samples were characterised at room temperature with *I-V* and *C-V* measurements, performed by an HP 4140 B pA meter/DC voltage source and an HP 4192A LF Impedance Analyzer, respectively. Hereafter, the sample was placed in a closed cycle helium cryostat and characterised by conventional DLTS.

3. Results and discussion

3.1. I-V and C-V characteristics

The devices were tested from *I-V* and *C-V* measurement systems to determine the quality of diodes before in between irradiations. Fig. 1 shows the forward semi-logarithmic *I-V* characteristics of the SBD measured at 300 K for un-irradiated to the radiation fluence of 7.9×10^{11} cm^{-2}. For biases below approximately 1 V, where thermionic emission dominates, a slight increase in forward current was observed as a result of increase in radiation fluence. The ideality factor was 1.20 for the as-deposited sample and increased to 1.85 after 9.2×10^{11} cm^{-2} bombardment. This confirms that the current transport mechanism at low fluence was dominated by thermionic emission. The increase in ideality factor at higher fluences indicates that, in addition to thermionic emission, other transport mechanisms might also contribute. Barrier height inhomogeneiety might also play a role. The Schottky barrier height ($\phi_{b, I\text{-}V}$)

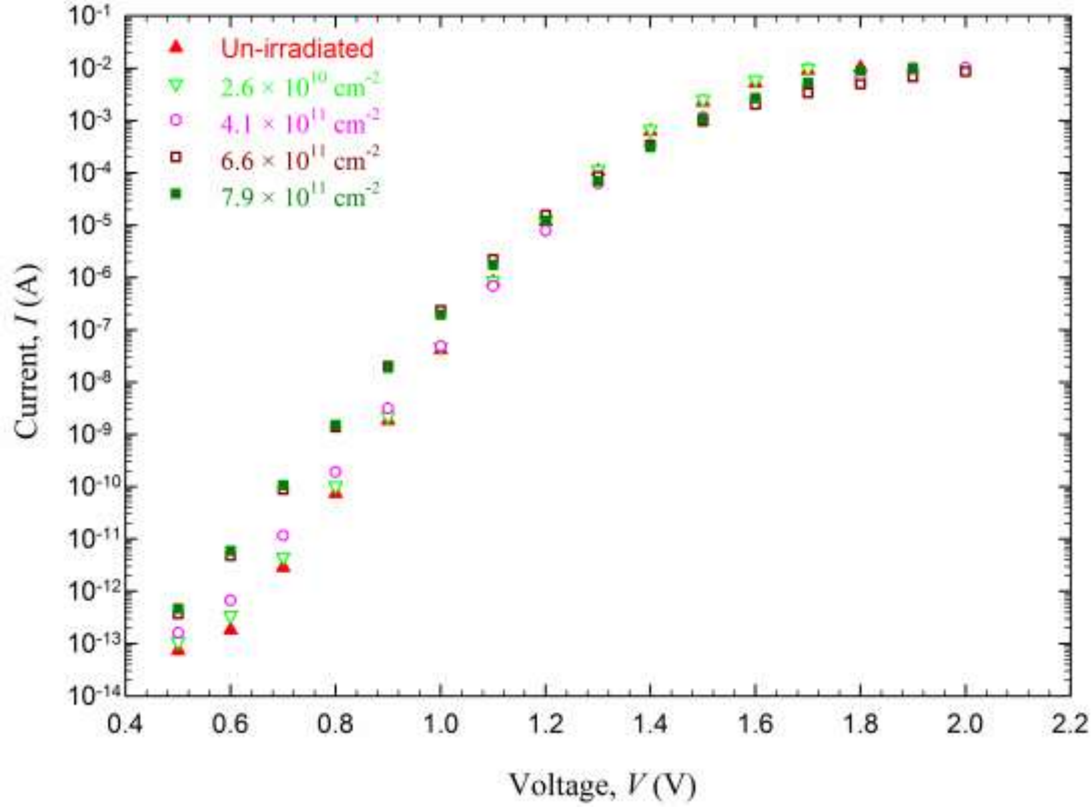

Fig. 1. Forward *I-V* characteristics of 4H-SiC SBD before and after5.4 MeV alpha-particle irradiation up to fluence 7.9×10^{11} cm^{-2} measured at 300 K.

decreased with increasing irradiation fluence (1.47 - 1.34) eV and saturation current also increased with fluence from 2.3×10^{-21} to 5.2×10^{-19} A. The fluence dependency of the n, $\phi_{b, I\text{-}V}$ and I_s may also connected with the movement (shift) of Fermi level pinning at the surface of SiC, since irradiation-induced defects can creates interface states. The electrical parameters were determined as reported earlier by Omotoso *et al* [15, 16]. From these characteristics, it shows that 4H-SiC with doping density 1.9×10^{16} cm^{-3} is radiation hard compare to Si [17].

In Fig. 2, the leakage current is less than 1.8×10^{-10} A at reverse voltage (V_r) below 15.0 V for all the *I-V* measurements, starting from as deposited to the fluence of 7.9×10^{11} alpha-particles-cm^{-2}. From Table 1, as the reverse bias increased, an increase in leakage current was observed before and after irradiation. But, contrary to the case in other semiconductors, the leakage current decreased with increase in radiation fluence. This occurs despite a decrease observed in the forward barrier height. A possible explanation would be that the decrease in leakage current is related to the decrease in free carrier density caused by the introduction of compensating defects. This would, in turn, decrease the electric field in the depletion region.

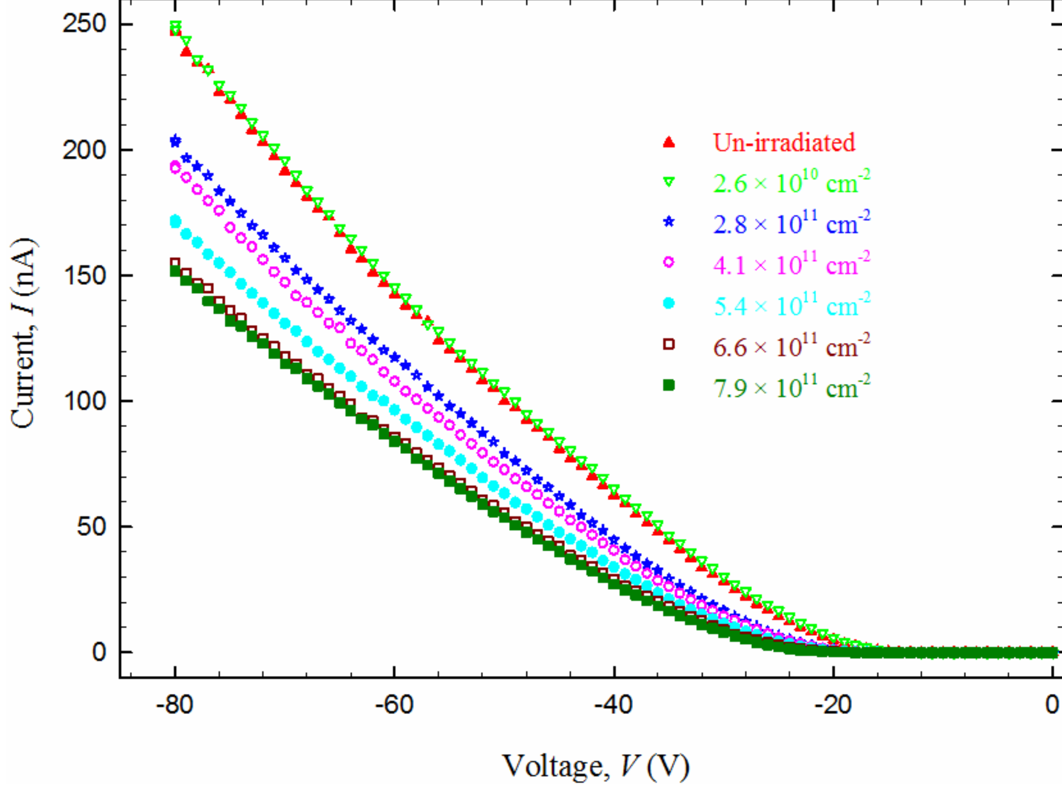

Fig. 2. Semi-logarithmic curves of the reverse leakage current measured up to –80 V as a function reverse voltage measured at fluence ranges from 2.6×10^{10} cm^{-2} to 7.9×10^{11} cm^{-2}.

Table 1
Comparison of leakage current and reverse voltage in a Ni/4H-SiC SBD before and after irradiation with alpha-particles.

Reverse voltage (V)	Leakage current (nA)	
	Un-irradiated	At fluence of 7.9×10^{11} cm^{-2}
40	64	27
60	143	85
80	247	153

Three possible reverse conduction mechanisms were considered: Thermionic emission (with image force barrier lowering), thermionic-field emission (tunnelling) and impact ionization. All three mechanisms predict that a reduction in the electric field in the barrier would reduce the reverse current.

The C^{-2} as a function of reverse bias voltage, V before and after step-wise irradiation of the samples at fluences ranges from 2.6×10^{10} to 9.2×10^{11} cm^{-2}, measured at 1 MHz are depicted in Fig. 3. From the C-V measurements, the free carrier concentrations, N_d, and the Schottky barrier heights, $\phi_{b, C\text{-}V}$, were calculated from

$$N_d = \frac{2}{q\varepsilon_s A^2}\frac{d\left(1/_{C^2}\right)}{dV} \quad (1)$$

$$\Phi_{b,C-V} = V_{bi} + \frac{kT}{q} + \xi \quad (2)$$

and $x = \varepsilon_s A/C$ is the depletion width of the space charge region, C is the capacitance, V_{bi} is the built-in voltage, k is the Boltzmann constant, T is the temperature, q is the electron charge, ε_{s} is the permittivity of semiconductor, A is the area of the diode and ξ is the difference between conduction band and the Fermi level.

The capacitance of the sample decreased with increase in radiation fluence. At a reverse bias of –5 V, the capacitance obtained before and after irradiation at fluence 9.2×10^{10} cm^{-2} was 34.9 and 25.6 pF, respectively. The decrease in capacitance of the diodes with irradiation is probably as a result of the semiconductor depletion width increasing due to the introduction of defects with acceptor states in the band gap, reducing the free carrier concentration of the SBD after irradiation. The change in capacitance may also attributed to change in dielectric constant at the interface, however this effect should be negligible as the interfacial layer is very thin. Furthermore, the reduction in free carrier concentration was also observed in the slope of the C^{-2} versus V plot. As shown in Table 2, the SBH for I-V and C-V did not agree. This could be due to the different approach of the measurement techniques. C-V measurement is not a transport technique. This may also be as a result of inhomogeneous Schottky barrier diodes.

Table 2
Summary of important parameters before and after bombardment of Ni/4H-SiC SBDs with fluence 9.2×10^{11} cm^{-2} from a 241-Am radionuclide source, calculated from I-V and C-V characteristics. C-V characteristics were determined at depletion width of 0.7 µm.

Sample	n	$\phi_{b,\,I\text{-}V}$ (eV)	$\phi_{b,\,C\text{-}V}$ (eV)	I_s (A)	N_d (cm^{-3})	C (pF) at –5 V
Un-irradiated	1.20	1.47	2.44	2.3×10^{-21}	1.6×10^{16}	34.9
9.2×10^{11} cm^{-2}	1.85	1.34	3.66	5.2×10^{-19}	1.1×10^{16}	25.6

From Fig. 3, the free carrier concentrations, $N_{\mathrm{d}} - N_{\mathrm{a}}$ were determined from the slope of the plots C^{-2} versus V. The free carrier concentration of the sample decreases with increase in radiation fluence. The $N_{\mathrm{d}} - N_{\mathrm{a}}$ for the diodes before irradiation and after bombardment with fluence 9.2×10^{10} cm^{-2} were 1.6×10^{16} and 1.1×10^{16} cm^{-3}, respectively. An indication that defects were introduced during the irradiation caused the reduction in the free carrier concentration. It is proposed that these defects are vacancy related. These also have the effect of compensating the free carriers. The change in free carrier concentration of active defect at

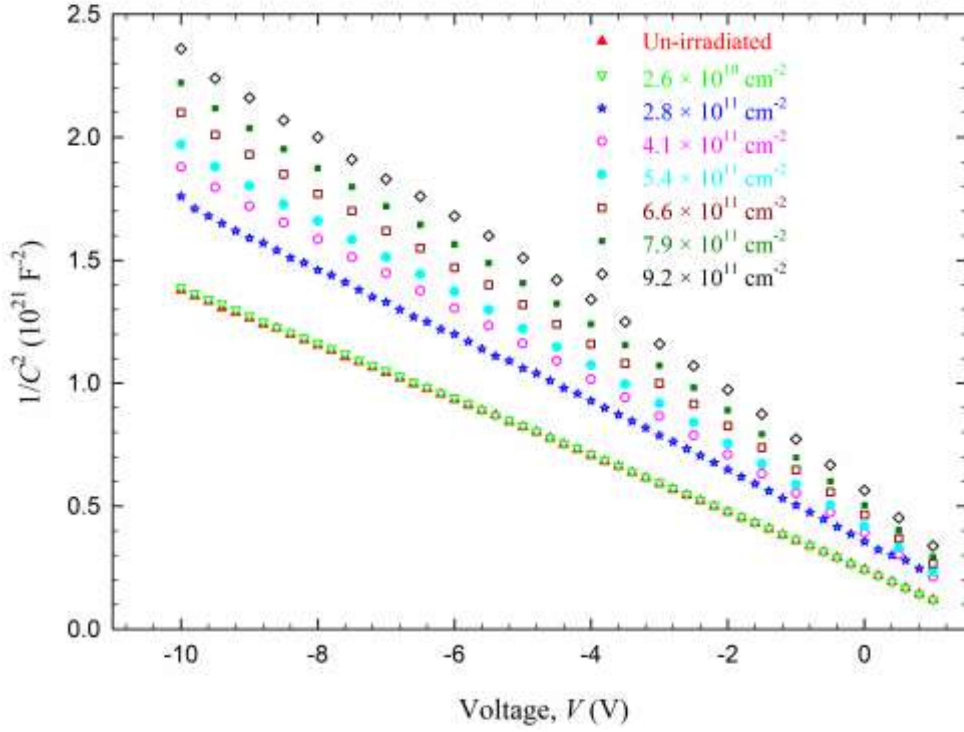

Fig. 3. $1/C^2$ as a function of voltage characteristics of 4H-SiC SBDs before and after 5.4 MeV alpha-particle irradiation at fluence ranges 2.6×10^{10} cm^{-2} to 9.2×10^{11} cm^{-2}.

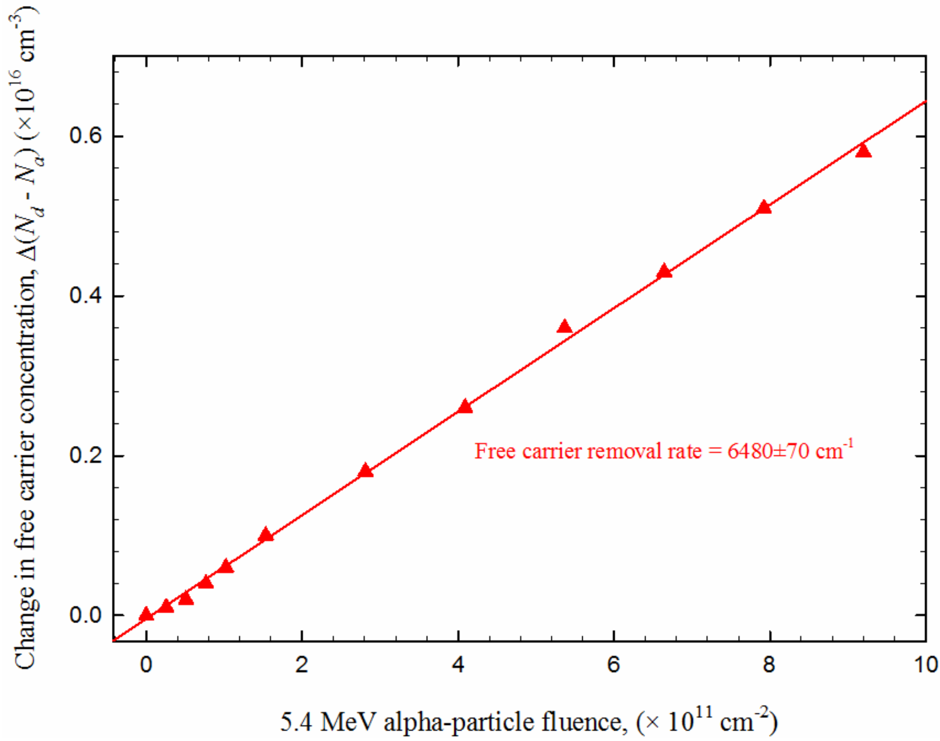

Fig. 4. The change in free carrier concentration of a 4H-SiC SBD after 5.4 MeV alpha-particle irradiation as a function of fluence. The free carrier concentration values were obtained at depth 0.7 μm below the metal-semiconductor interface.

a depletion width of approximately 0.70 μm from the interface, as function of radiation fluence, is shown in Fig. 4. The free carrier removal rate, η can be obtained from Eq. 3 below:

$$\eta = \frac{\Delta(N_d - N_a)}{\varphi} \qquad (3)$$

where $\Delta(N_d - N_a)$ is the change in free carrier concentration, φ is the fluence at which the sample was bombarded [18]. The graph of $\Delta(N_d - N_a)$ against the corresponding fluence received by the sample was plotted. The free carrier removal rate was determined to be 6480±70 cm^{-1} from the slope of the plot. This value is two orders of magnitude less than the value for Si reported by Kozlovski *et al* who determined a free carrier removal rate of 4×10^5 cm^{-1} in Si with an initial free carrier concentration of 1×10^{15} cm^{-3} irradiated by 1.7 MeV alpha-particle at a fluence of 2×10^9 cm^{-2} [19].

From the results of both *I-V* and *C-V* characteristics at different fluences, it is apparent that the diodes were of a reasonable electrical quality and were suitable for the analysis of DLTS.

3.2. Deep level transient spectroscopy analysis

Fig. 5 shows the normalized DLTS spectra of the devices before and after step-wise bombardment with 5.4 MeV from a 241-Am radionuclide source with fluence ranges from 2.56×10^{10} to 9.20×10^{11} cm^{-2} at rate window of 200 s^{-1}. The measurements were obtained over the temperature range 22 – 350 K, at a quiescent reverse bias of −5.0 V, filling pulse of amplitude 6.0 V and width 2.0 ms and at different rate windows (2.5 to 1000 s^{-1}). Fig. 6 shows the Arrhenius plot of the defects observed before and after the step-wise bombardment. The *signatures* of the defects in terms of activation energy E_n and apparent capture cross section, σ_n were determined from Fig. 6. The activation energy of each defect was determined from the slope, and the corresponding apparent capture cross section was calculated from the intercept of the Arrhenius plot of log (T^2/e_n) versus $1/T$ as earlier reported by Auret *et al* [20]. Four deep levels labelled $E_{0.09}$, $E_{0.11}$, $E_{0.16}$ and $E_{0.65}$ (where 'E' refers to an electron trap and the subscript 0.09 refers to an energy level below the conduction band), were present before irradiation as previously observed by Omotoso *et al* [21]. After the sample was bombarded, it was observed that two defects were introduced by irradiation. One of the defects had a broad peak, probably due to the presence of several states or defects with closely spaced emission rates as observed earlier [22]. The irradiation induced defects were labelled as $E_{0.39}$ and $E_{0.62}$. The electronic properties of the deep levels labelled $E_{0.09}$, $E_{0.11}$, $E_{0.16}$, $E_{0.62}$ and $E_{0.65}$ have been presented by Omotoso *et al* [21]. The activation energy and apparent capture cross section of $E_{0.39}$ after fluence 9.2×10^{11} cm^{-2} are 0.39±0.03 and 1.7 ×

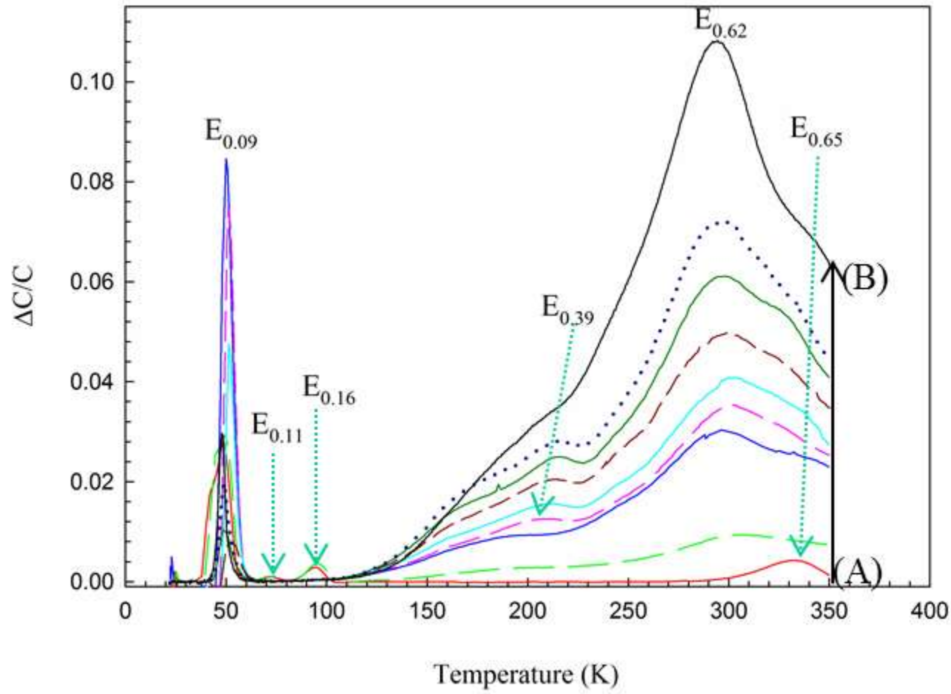

Fig. 5. Normalized DLTS spectra of 4H-SiC before and after irradiation at radiation fluence ranges from 2.6×10^{10} cm^{-2} to 9.2×10^{11} cm^{-2} at rate window of 200 s^{-1}. *Line A to B represents from un-irradiated to* 2.6×10^{10}, 2.8×10^{11}, 4.1×10^{11}, 5.4×10^{11}, 6.6×10^{11}, 7.9×10^{11}, 9.2×10^{11} cm^{-2} *to 1 week after* 9.2×10^{11} cm^{-2}, *spectra.*

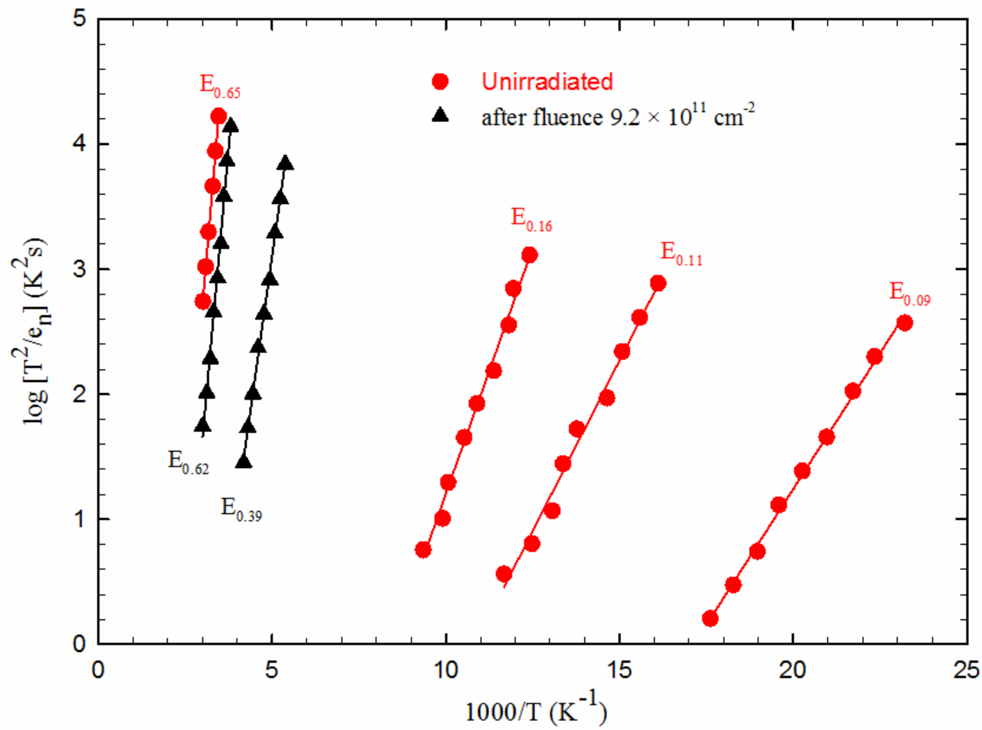

Fig. 6. Arrhenius plots for defects n-type 4H-SiC observed before and after irradiation with 5.4 MeV alpha-particles irradiation at fluence 9.2×10^{11} cm^{-2}.

10^{-15} cm^2, respectively. As the two emanated defects becoming conspicuous, the intensity of $E_{0.09}$, $E_{0.11}$ and $E_{0.16}$ reduced. The defects, $E_{0.11}$ and $E_{0.16}$ disappeared after irradiation to a fluence of 4.1×10^{11} cm^{-2}. After receiving irradiation to a fluence of 9.2×10^{11} cm^{-2}, the $E_{0.09}$ reduced to 12% of its intensity before irradiation.

Table 3
Electronic properties of defects detected by DLTS in Ni/4H-SiC SBD before and after bombarded with fluence of 9.2×10^{11} alpha-particles-cm^{-2}.

Defect	E_T (eV)	σ_a (cm^2)	T_{peak} (K)	Attribution
$E_{0.09}$	E_c–0.09	8×10^{-15}	51	N impurity [30]
$E_{0.11}$	E_c–0.11	2×10^{-16}	74	Ti impurity [31]
$E_{0.16}$	E_c–0.16	1×10^{-15}	94	Ti impurity [27]
$E_{0.39}$	E_c–0.39	2×10^{-15}	217	V_{Si} [23]
$E_{0.62}$	E_c–0.62	1×10^{-13}	301	Z_1/Z_2 [30, 32]
$E_{0.65}$	E_c–0.65	4×10^{-15}	332	Z_1/Z_2 (C/Si vacancy [27, 28])

NOTE: The T_{peak}(K) was taken at rate window of 200 s^{-1}

Table 3 shows the attributes of each defect. A defect similar to $E_{0.39}$ showing acceptor-like behaviour, was reported earlier after electron irradiation by Doyle *et al* [23]. From Fig. 4, the decrease in the free carrier concentration indicates an increase in compensation with radiation fluence which suggests the acceptor-like behaviour of deep levels introduced into the device. A similar defect level has been attributed to the silicon vacancy [24], carbon vacancy, split interstitial or antisites after low energy electron irradiation [25]. It was observed that defect $E_{0.39}$ disappeared after leaving the sample at room temperature for a week, showing that the defect was not stable at room temperature. The deep level defects $E_{0.62}$ and $E_{0.65}$ have been previously reported to be defects composed of several energy levels commonly referred to as the Z_1/Z_2 [16, 26-29].

4. Conclusions

In summary, the effect of alpha-particle irradiation at different fluences resulted in a decrease in leakage current from 64 nA (for un-irradiated) to 27 nA (fluence of 9.2×10^{11} cm^{-2}) at reverse voltage of 40 V. The decrease was attributed to a reduction in the electric field in the depletion region due to a reduction in the space charge density because of compensating acceptors introduced during irradiation. A reduced electric field would explain lower reverse current for a number of current transport mechanisms including thermionic emission with image force barrier lowering, thermionic-field emission (tunnelling) and

impact ionization. For forward conduction, thermionic emission was dominant at lower fluence, while deviations were observed after irradiation at higher fluence.

The capacitance of diodes decreased with increase in radiation fluence as a result of increase in the depletion width due to reduction in free carrier concentration of the SBD after irradiation.

Our DLTS results revealed the presence of four electron deep levels before irradiation with energy levels labelled $E_{0.09}$, $E_{0.11}$, $E_{0.16}$ and $E_{0.65}$. Alpha-particle irradiation at fluence ranges from 2.56×10^{10} to 9.2×10^{11} cm^{-2} induced two broad electron defects with energies E_c–0.39 and E_c–0.62, respectively. The presence of broad peak indicates presence of several states or defects with close activation energies. The defect $E_{0.39}$ showed an acceptor-like behaviour and can be attributed to be a silicon or carbon vacancy. It was observed that defect $E_{0.39}$ disappeared after leaving the sample at room temperature for a week. The deep level defects $E_{0.62}$ and $E_{0.65}$ are widely agreed to be intrinsic in nature and commonly referred to as the Z_1/Z_2 defect.

Acknowledgements

This work is based on the research supported in part by the National Research Foundation (NRF) of South African (Grant specific unique reference number (UID) 78838). The Grant holder acknowledges that opinions, findings and conclusions or recommendations expressed in this publication generated by the NRF supported are that of authors and that NRF accepts no liability whatsoever in this regard.

References

[1] R.L. Van Tuyl, C.A. Liechti, Solid-State Circuits, IEEE Journal of, 9 (1974) 269-276.
[2] A. Elasser, M.H. Kheraluwala, M. Ghezzo, R.L. Steigerwald, N.A. Evers, J. Kretchmer, T.P. Chow, Industry Applications, IEEE Transactions on, 39 (2003) 915-921.
[3] S. Takayuki, U. Tsuneo, S. Seizo, M. Yoshihiko, Japanese Journal of Applied Physics, 19 (1980) 459.
[4] A.F. Özdemir, A. Turut, A. Kökçe, Semiconductor Science and Technology, 21 (2006) 298.
[5] E. Rhoderick, R. Williams, Oxford Science, Oxford, 1988.
[6] V. Janardhanam, A. Ashok Kumar, V. Rajagopal Reddy, P. Narasimha Reddy, Journal of Alloys and Compounds, 485 (2009) 467-472.
[7] L.M. Tolbert, B. Ozpineci, S.K. Islam, M.S. Chinthavali, Power and Energy Systems, Proceedings, 1 (2003) 317-321.
[8] M. Siad, M. Abdesslam, A.C. Chami, Applied Surface Science, 258 (2012) 6819-6822.
[9] R. Madar, Nature, 430 (2004) 974-975.
[10] S. Yamada, B.-S. Song, T. Asano, S. Noda, Applied Physics Letters, 99 (2011) 2011021-2011023.
[11] T. Nishijima, T. Ohshima, K.K. Lee, Nuclear Instruments and Methods in Physics Research Section B: Beam Interactions with Materials and Atoms, 190 (2002) 329-334.

[12] F. Nava, E. Vittone, P. Vanni, G. Verzellesi, P.G. Fuochi, C. Lanzieri, M. Glaser, Nuclear Instruments and Methods in Physics Research Section A: Accelerators, Spectrometers, Detectors and Associated Equipment, 505 (2003) 645-655.
[13] L. Kin Kiong, T. Ohshima, H. Itoh, Nuclear Science, IEEE Transactions on, 50 (2003) 194-200.
[14] T. Marinova, A. Kakanakova-Georgieva, V. Krastev, R. Kakanakov, M. Neshev, L. Kassamakova, O. Noblanc, C. Arnodo, S. Cassette, C. Brylinski, B. Pecz, G. Radnoczi, G. Vincze, Materials Science and Engineering: B, 46 (1997) 223-226.
[15] E. Omotoso, W.E. Meyer, F.D. Auret, A.T. Paradzah, M. Diale, S.M.M. Coelho, P.J. Janse van Rensburg, Materials Science in Semiconductor Processing, 39 (2015) 112-118.
[16] E. Omotoso, W.E. Meyer, F.D. Auret, A.T. Paradzah, M. Diale, S.M.M. Coelho, P.J. Janse van Rensburg, P.N.M. Ngoepe, Nuclear Instruments and Methods in Physics Research Section B: Beam Interactions with Materials and Atoms, (2015) 5.
[17] A.A. Lebedev, V.V. Kozlovski, Semiconductors, 48 (2014) 1293-1295.
[18] F. Auret, S. Goodman, M. Hayes, M. Legodi, H. Van Laarhoven, D.C. Look, Applied Physics Letters, 79 (2001) 3074-3076.
[19] V. Kozlovski, V. Abrosimova, International journal of high speed electronics and systems, 15 (2005) 1-253.
[20] F.D. Auret, P.N.K. Deenapanray, Critical Reviews in Solid State and Materials Sciences, 29 (2004) 1-44.
[21] E. Omotoso, W.E. Meyer, F.D. Auret, A.P. Paradzah, M. Diale, S.M.M. Coelho, P.J. Janse Van Rensberg, Nuclear Instruments and Methods in Physics Research Section B: Beam Interactions with Materials and Atoms, submitted for publication.
[22] Ž. Pastuović, I. Capan, D.D. Cohen, J. Forneris, N. Iwamoto, T. Ohshima, R. Siegele, N. Hoshino, H. Tsuchida, Nuclear Instruments and Methods in Physics Research Section B: Beam Interactions with Materials and Atoms.
[23] J. Doyle, M.K. Linnarsson, P. Pellegrino, N. Keskitalo, B. Svensson, A. Schoner, N. Nordell, J. Lindstrom, Journal of applied physics, 84 (1998) 1354-1357.
[24] F. Nava, G. Bertuccio, A. Cavallini, E. Vittone, Measurement Science and Technology, 19 (2008) 102001.
[25] L. Storasta, J.P. Bergman, E. Janzén, A. Henry, J. Lu, Journal of Applied Physics, 96 (2004) 4909-4915.
[26] T.A.G. Eberlein, R. Jones, P.R. Briddon, Physical Review Letters, 90 (2003) 2255021-2255024.
[27] T. Dalibor, G. Pensl, H. Matsunami, T. Kimoto, W.J. Choyke, A. Schöner, N. Nordell, physica status solidi (a), 162 (1997) 199-225.
[28] I. Pintilie, L. Pintilie, K. Irmscher, B. Thomas, Applied Physics Letters, 81 (2002) 4841-4843.
[29] A.T. Paradzah, F.D. Auret, M.J. Legodi, E. Omotoso, M. Diale, Nuclear Instruments and Methods in Physics Research Section B: Beam Interactions with Materials and Atoms, 358 (2015) 112-116.
[30] T. Kimoto, A. Itoh, H. Matsunami, S. Sridhara, L. Clemen, R. Devaty, W. Choyke, T. Dalibor, C. Peppermüller, G. Pensl, Applied physics letters, 67 (1995) 2833-2835.
[31] A.A. Lebedev, Semiconductors, 33 (1999) 107-130.
[32] G. Pensl, W.J. Choyke, Physica B: Condensed Matter, 185 (1993) 264-283.